Int. J. Electrochem. Sci., 12 **(2017)** 10447 – 10456, doi: 10.20964/2017.11.43

International Journal of ELECTROCHEMICAL SCIENCE
www.electrochemsci.org

Short Communication

Glancing Angle Deposited Pt Nanorod Array Electrocatalysts for Direct Ethanol Fuel Cells

Wisam J. Khudhayer[1,*] , *Ali S. Allw*[1], *Mohammed D. Salman*[2] , *Tansel Karabacak*[3]

[1] Department of Energy Engineering, College of Engineering / Al-Musayab, University of Babylon, Hillah 51002, IRAQ
[2] College of Engineering, University of ThiQar, ThiQar 64001, Iraq
[3] Department of Applied Science, University of Arkansas at Little Rock, Little Rock, Arkansas 72204, USA
[*]E-mail: Met.Wisam.j@uobabylon.edu.iq

Received: 12 November 2015 / *Accepted:* 22 August 2017 / *Published:* 12 October 2017

The catalytic activity of vertically aligned platinum nanorod arrays for ethanol electrooxidation has been evaluated utilizing cyclic voltammetry (CV) in 0.5 M H_2SO_4 and 0.5 M ethanol electrolyte at room temperature. The Pt nanorods electrodes were grown using a magnetron sputtering glancing angle deposition (GLAD) technique at different lengths (400 ad 600 nm long). The x-ray diffraction and SEM results reveal that that Pt nanorod are well-isolated, single crystal, and mainly oriented in Pt(100) which has the highest activity for ethanol adsorption and electrooxidation. The CV results show that the forward anodic current density (I_f) to the reverse anodic peak current density (I_b) ratio is calculated to be 4.8 and 7.2 for 400 and 600 nm Pt nanorods, respectively, while it is around 2.5 for a commercial high-surface-area-supported Pt (Pt/C) catalyst. Such high ratio for Pt nanorods electrocatalysts reflects the enhanced tolerance to the accumulation of carbonaceous species; a larger quantity of intermediate carbonaceous species is converted (oxidized) to CO_2 in the forward scan compared to Pt/C, thus significantly enhancing the electrode electroactivity.

Keywords: Glancing Angle Deposition (GLAD) technique, GLAD Pt nanorod arrays electrocatalysts, Electrooxidation of Ethanol, Direct Ethanol Fuel Cells.

1. INTRODUCTION

There is a great interest in the development of direct alcohol fuel cell (DAFC) due to its potential applications in the electrical vehicles and portable electronic devices [1,2]. One of the most electro-active alcohol fuels is methanol, which has a variety of advantages such as high energy density, availability, low price, and the easiness of its storage and refilling. However, its toxicity and possible environmental problems related to its large miscibility to water initiate the need for finding alternative

fuels. This is in addition to its crossover from anode to cathode through polymer electrolyte membrane leading to low system efficiency [3]. As an alternative, ethanol is an attractive fuel due to its higher energy density and lower toxicity than methanol. This is in addition to the fact that it can be produced from renewable sources in large quantities [3]. However, it is well known that the complete oxidation of ethanol is more difficult than that of methanol [1-3]. The main challenge in achieving an efficient conversion at low overpotential is that the electro-oxidation of ethanol follows different reaction pathways. In some pathways, the difficulty in rupturing C-C bond results in large amounts of partially oxidized products. The acetaldehyde and acetic acid or acetate are the main partially oxidized products, which do not only result in decreasing the total efficiency of the system, but are also unwanted products due to their polluting nature. In other pathways, strongly adsorbed species such as CO and carbohydrate (CH_x) fragments are formed, which are always considered as one of the main poisoning species of the platinum catalyst surface at low operating temperature [4]. It should be noted that the dissociative adsorption of the organic molecules is the origin of the above-adsorbed species [1-5]. In order to handle this issue, it is necessary to alter the composition, structure of the anode electrocatalysts and electrode surface so that, at low potential, the electrode surface coverage in oxygenated species (such as adsorbed OH), coming from the dissociative adsorption of water, will be increased. These OH species are necessary for the complete oxidation of the species coming from the dissociation of alcohols to CO_2 at low potentials [5].

Although different carbon-supported Pt or Pt-based alloys electrocatalysts were suggested for ethanol electro-oxidation only PtRu and PtSn with optimized compositions and structures are found to be the most active electrocatalysts compared to others [6-8]. However, some detailed studies have shown that the incomplete oxidation products such as acetaldehyde and acetic acid were still the main reaction products on PtSn/C and PtRu/C catalysts, added to the formation of small amount of CO_2 [6-9]. This is an indication that the complete ethanol oxidation on PtSn/C and PtRu/C was suppressed. Some recent studies [10-13] have focused on ternary Pt-based electrocatalysts, which are expected to give more flexibility in tuning geometric and electronic properties of Pt surfaces, leading to a higher electrocatalytic performance [8,11].

One of the most active electrocatalysts is the ternary $PtRhSnO_2/C$ electrocatalysts, which were synthesized by the cation-adsorption-reduction-galvanic-displacement method. This method includes depositing of Pt and Rh atoms on carbon-supported tin oxide nanoparticles using a controllable deposition of metal atoms on oxide surfaces [10]. This electrocatalyst exhibits a remarkable enhance in ethanol electro-oxidation; the electrochemical activity of $PtRhSnO_2/C$ is ~100 times higher than that of Pt/C [10]. This electrocatalysts facilities the ethanol oxidation to CO_2 at low potential by effectively breaking the C-C bond in ethanol at room temperature in acid solutions, which has not been achieved with the existing catalysts [8]. The high electrochemical activity of $PtRhSnO_2/C$ is attributed to the specific property of each of its constituents, induced by their interaction. For example, Rh promotes ethanol oxidation kinetics at anode in DEFCs due to an enhanced ethanol oxidation mechanism that occurs through an oxametallacyclic (CH_2CH_2O) conformation that then facilitates the direct rupture of the C-C bond at an acceptable rate. On the other hand, SnO_2 is playing an important role in facilitating C-C bond cleavage by altering the electronic structure of Rh so that it can afford moderate bonding to ethanol, intermediates, and products [10]. It also has the ability to strongly adsorb water and interact

with Pt and Rh deposited on its surface, apparently prevents the Pt and Rh sites from reacting with water to form M-OH, thus allowing these sites to be available for ethanol electro-oxidation [10]. The dissociated CO at Rh sites can be oxidized by the OH species provided by SnO_2 with water and Pt facilitates ethanol dehydrogenation. It should be noted that the incomplete oxidation products on $PtRhSnO_2/C$ are still produced but their production rates are minimized compared to the existing conventional electrocatalysts. Recently, Adzic and co-workers have replaced Rh by Ir and they have reported that the Ir-containing electrocatalysts with high Ir content shows outstanding catalytic activity [11]. However, the approach that has been used to fabricate such ternary electrocatalysts includes a multi-step, complicated, and time-consuming process. Moreover and as described in our previous studies [14,15], the carbon support causes additional challenges, including carbon oxidation, the formation of peroxide species that leads to the degradation of the polymeric membrane, and the separation of carbon over time from the ionomer, leading to the loss of the electrochemical active surface area (ECA) of the catalyst.

More recently, Abruna and co-workers [13] have studied 91 combinations of Pt-Sn-M electrocatalysts and they concluded that the variation and combination of different components could enhance the electro-oxidation activity of ethanol to CO_2 with different electronic effects. Based on what has been presented above, in the present work, we propose a new multifunctional electrode design comprised of a single layer and carbon-free catalyst nanorod arrays with extremely low Pt loadings, unique crystal properties, enhanced electrochemical activity for ethanol oxidation reaction. Catalyst nanorods will be made from a) Elemental Pt and b) SnO_2 nanorods, which are partially coated with Pt and Rh or Ir atoms on the surface to enhance ethanol oxidation at the anode side in DEFCs.

The first step of our research plan has been carried out by fabricating vertically aligned Pt catalyst nanorod arrays with different lengths of 400 and 600 nm, which correspond to 0.32-0.5 mg/cm^2 Pt loadings, utilizing the glancing angle deposition (GLAD) technique. The electrochemical activity of the samples has been evaluated as an anode for ethanol oxidation in an acidic environment compared to the conventional Pt/C electrocatalyst. The GLAD technique offers a novel capability for fabricating nanostructured thin films of various materials (pure elements, alloys, compounds, and oxides) with interesting properties [14-19]. It is a simple, single-step, cost and time efficient technique, which uses the “shadowing effect,” to grow isolated 3D nanostructures. The "shadowing effect" is a physical self-assembly process, which promotes the preferential growth on the islands of higher height on the substrate. During GLAD, some islands grow faster in the vertical direction, then they started to capture the obliquely incident atoms, while the shorter islands get shadowed and cannot grow any more, leading to the formation of isolated nanostructures. By utilizing GLAD technique, the multicomponent nanostructures can be grown by using multiple sources/targets of materials in the deposition systems [15,16].

2. EXPERIMENTAL WORK

The DC magnetron sputter GLAD technique (Excel Instruments, India) was used for growing vertically aligned Pt nanorod arrays for different growth times of 60 and 80 minutes, which correspond to 400 and 600 nm long Pt nanorods. Figure 1 shows the schematic of the GLAD experimental setup.

The Pt nanorods were deposited at a glancing angle of $\theta = 85^{o}$ (with respect to the substrate normal) on flat Pt thin film coated silicon substrates, which were rotated around the surface normal with a speed of 2 rpm. The distance between the substrates and the sputter target (99.99% pure Pt disk-shaped source with 2.54 cm in diameter) was approximately 12 cm. In order to achieve a base pressure of about 2.4×10^{-6} Torr, a turbo-molecular pump backed by a mechanical pump were used. During the GLAD depositions, a DC power supply was used to generate the plasma for the Pt target with a power of 150 Watts with an ultra-pure Argon working gas pressure of 2.4×10^{-3} Torr. In order to avoid the delamination issue during the electrochemical tests, a thin layer of chromium was deposited as an adhesion layer to the silicon substrate prior to Pt film deposition. The quartz crystal microbalance (QCM) measurements as well as the analysis of the cross-sectional SEM images were utilized to measure the deposition rate of the GLAD Pt nanorods to be approximately 7.5 nm/min. By controlling the deposition rate and deposition time, we can set the length of the rods to values from a few nanometers up to the micrometer range.

As described in our previous studies [14-17], the weight loadings of Pt nanorods were measured using our quartz crystal microbalance (QCM, Inficon-Q-pod QCM monitor, crystal: 6 MHz gold coated standard quartz) set-up. For this purpose, we deposited GLAD Pt nanorods directly on QCM crystals and measured the loading values by comparing the oscillation frequencies of the blank and coated crystal. The surface morphology and crystallographic structure of Pt nanorods have been investigated using scanning electron microscopy (SEM) unit (FESEM-6330F, JEOL Ltd, Tokyo, Japan) and X-ray diffraction (XRD) system (Bruker D8 discover), respectively.

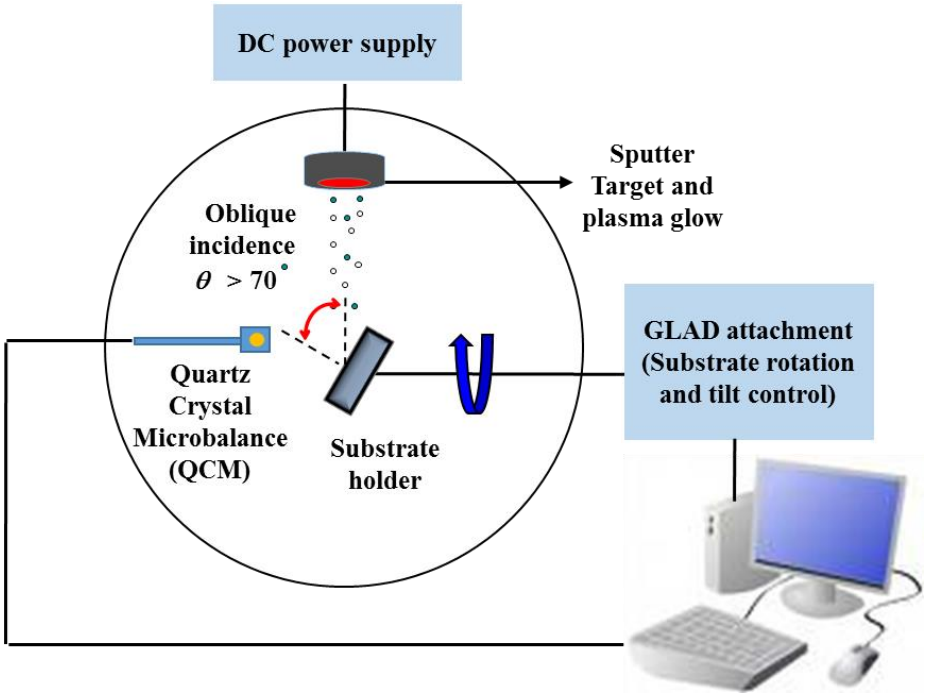

Figure 1. A schematic of the glancing angle deposition (GLAD) experimental setup used for the fabrication of vertically aligned Pt nanorod arrays. The Pt nanorods were deposited at a glancing angle of 85^{o} (with respect to the surface normal) and the substrates were rotated around the surface normal with a speed of 2 rpm.

For electrochemical property comparison to Pt nanorods, the conventional carbon-supported Pt nanoparticle electrode (Pt/C 20 wt% Pt on carbon black, Clean Fuel Cell Energy, LLC) was prepared as described by Wisam et al. [14]. Briefly, 20 ml of isopropanol with 79.6 ml of DI water, and 0.4 ml of 5% Nafion ionomer solution (Clean Fuel Cell Energy, LLC) were mixed to prepare a stock solution of 20% isopropanol and 0.02% Nafion ionomer. Ten milligrams of the Pt/C catalyst were mixed with 5 milliliter of the stock isopropanol/Nafion solution using an ultrasonicator. A glassy carbon rotating disk electrode was electrochemically cleaned, polished, and used as a substrate for 10 μL droplet of the well-dispersed catalyst ink, leading to a Pt loading of 20 μg Pt/cm^2. Finally, the catalyst ink-coated electrode was covered by a beaker to slow the solvent evaporation, resulting in smooth and crack-free films covering the entire surface of glassy carbon electrode. Based on the Pt loading on the glassy carbon substrate, the Nafion film thickness was found to be approximately less than 0.1 μm, which is in the range where diffusion effects within the thin film are considered negligible [20].

The electrochemical tests were performed at room temperature to characterize the catalyst electrocatalytic activity of the Pt nanorod arrays and Pt/C electrocatalysts. The electrochemical test setup was a typical three-electrode system, consisting of a working electrode, a counter electrode, and a reference electrode. As described above, 400 and 600 nm long GLAD Pt nanorods were deposited on flat Pt-film samples coated on Cr/Si wafer pieces. Pt film served as the continuous electrical-conducting layer, while Cr served to promote adhesion between the Pt film and Si substrate. Pt nanorods were set as a working electrode, and a platinum wire as a counter electrode located in a separate fritted compartment. The area of the working electrode samples were measured to be approximately ~0.20-0.36 cm^2. To ensure a maximum current density distribution through the working electrode, the area of the counter electrode was higher than that of the working electrode. A saturated calomel electrode (SCE) served as the reference electrode, and the electrolyte was a 0.5 M H_2SO_4 and 0.5 M ethanol solution, which was saturated by pure argon to exclude oxygen from the solution. This solution is analogous to the acidic electrolyte in DEFC fuel cells, Nafion® (Dupont). The CV experiments were performed using a Pine Instruments AFCBP1 Potentiostat with an in-built electrode unit. The working electrode samples were scanned from -300 to +1200 mV at a scan rate of 50 mV/seconds.

3. RESULTS AND DISCUSSION

3.1 Surface Morphology and Pt Loading Measurements

The top and side view SEM images of vertically aligned Pt nanorod arrays with different lengths are presented in Fig. 2. The isolated vertical columnar morphology of the nanorods can be clearly seen from the SEM images. The observed isolated morphology of the nanorods in lateral directions promotes a channeled porosity aligned in the vertical direction with respect to the substrate surface. This novel geometry can significantly enhance the effective transport of DEFC reactants to the catalyst sites in the electrode layer. Moreover, Fig. 2 shows that some of the nanorods have 6-fold symmetric faceted tips, indicating that an individual nanorod has a single crystal structure. This is in agreement with previous studies [21-25], in which it was reported that an individual metallic GLAD

nanorod is typically single crystal. The faceted sharp tips as well as the absence of the interior grain boundaries of the rods are expected to enhance electrocatalytic activity and reduce surface oxidation of the electrode layer in the fuel cell.

The QCM experimental unit was utilized for measuring the Pt loading of the electrodes. The Pt weight loadings were measured to be approximately 0.32 and 0.50 mg/cm^2 for 400 and 600 Pt nanorods, respectively. The QCM measurements reveals that the weight loading of Pt nanorods can be set to as low as 0.8 μg/cm^2 per nanometer length of the rods.

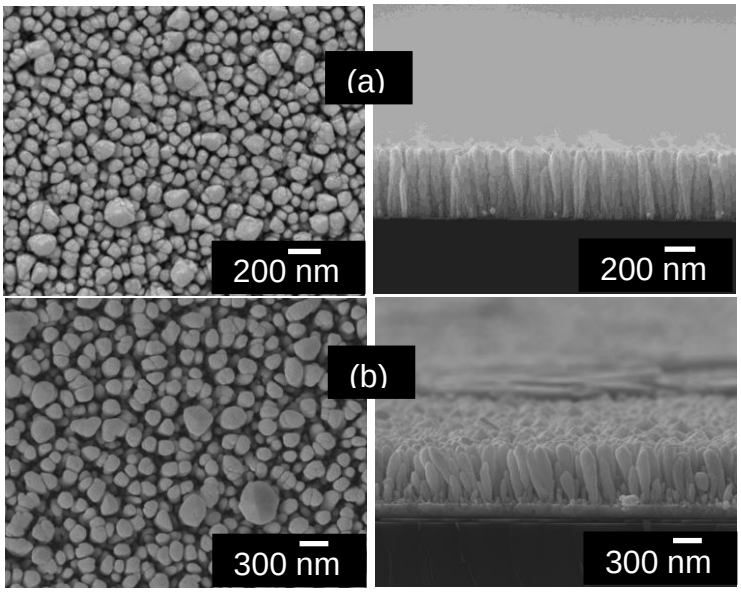

Figure 2. Top and side view scanning electron microscopy (SEM) images of vertically aligned GLAD Pt nanorod arrays of different lengths (a) 400, (b) 600 nm are shown. The deposition rate of GLAD Pt nanorods was determined to be approximately 7.5 nm/min.

3.2 Crystal Orientation Analysis

Figure 3 represents the XRD results, which demonstrate that Pt nanorods are mainly oriented in the (220) and (200) directions, which are the most active surfaces for anodic ethanol oxidation and cathodic oxygen reduction reaction (ORR). On the other hand, the polycrystalline Pt film is typically (111) texture, which is reported to be the energetically favorable growth plane of Pt films. The Pt(110) and Pt(100) orientations have higher electrochemical activity than that of Pt(111) plane. The poorer electrochemical activity of Pt(111) is caused by the relatively strong adsorption of bi-sulfate ions as reported in the previous studies [22, 25-27]. Furthermore, our results demonstrate that GLAD can be used to promote the Pt(100) growth between short nanorods (such as 20 nm with 0.025 mg/cm^2 Pt loading) to 400 nm Pt nanorods that have a higher electrochemical activity for both anodic (ethanol oxidation) and cathodic (ORR) than that of Pt(111). Ethanol adsorption and electrooxidation (anodic side in DEFCs) on Pt-based electrocatalyst was found to be a surface sensitive reaction [25]. It was reported that the formation of 1-C atom adsorbed species (CO) is a result of the splitting of the C-C bond, which occurs only to a limited extent [27]. The Pt(100) surface is showing the highest

electrochemical activity in this respect. Hence, the Pt(100) has a positive effect on both anodic and cathodic sides in DAFCs.

However, the trend of the dominance of Pt(100) is eventually reversed between 400 and 600 nm where Pt(110) becomes dominant over other crystal orientation, indicating the presence of another crystal orientation competition happening beyond 400 nm. This might be attributed to an increase in the number of the nanorods that are oriented in Pt(110) over those with dominant Pt(100). The Nanorods oriented in (110) direction become larger in diameter and higher in length so that they start to shadow other nanorods that are oriented in (100), and eventually become the dominant orientation. Therefore, other than deposition parameters listed above in the experimental section, texture of Pt nanorods can also be simply controlled by either through their length or by introducing a surface roughness as in the case of rough morphologies of GDL or membrane in DAFCs. Surface roughness together with the obliquely incident flux can control the shadowing effect during GLAD, which in turn can further promote the growth of energetically unfavorable but electrochemically more active crystal orientations. These results can pave the way to a better understanding of the fundamental relationship between the crystal orientation and the electrochemical activity.

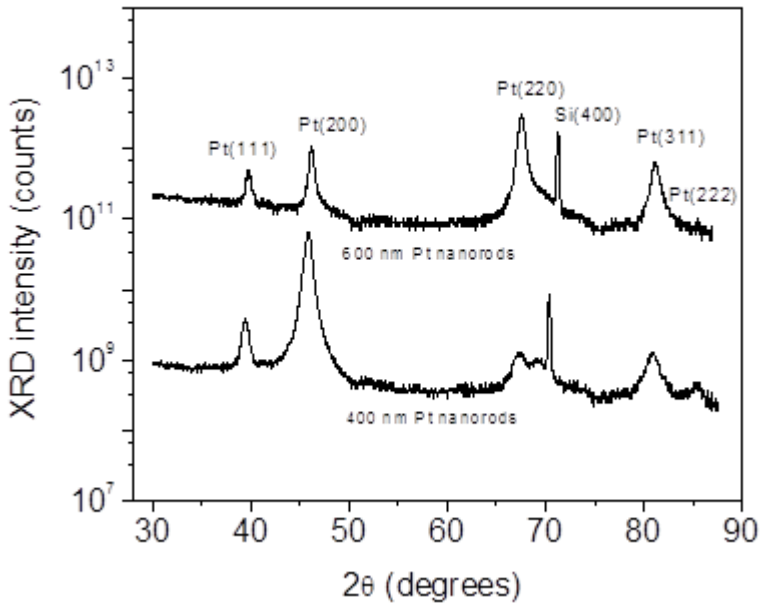

Figure 3. The X-ray diffraction (XRD) patterns of 400 and 600 nm long vertically aligned GLAD Pt nanorod arrays. Data is offset for clarity.

3.3 Electrochemical Characterization

The CV results of Pt/C, 400, and 600 nm long Pt nanorods electrocatalysts (Figs. 4a, b, and c, respectively) scanned between -300 and 1200 mV at a rate of 50 mV/s in a 0.5 M H_2SO_4 and 0.5 M ethanol solution are shown in Fig.4. In the investigated potential range, Fig. 4 reveals that there are two oxidation peaks for the electro-oxidation of ethanol. An oxidation peak of ethanol was detected at approximately ~0.72 mV in the forward scan for both Pt nanorods and Pt/C. While, in the reverse scan, the Pt nanorods and Pt/C catalysts exhibit an anodic peak at around 0.32 mV. The catalyst poisoning is

one of the most common problem in the electro-oxidation of ethanol due to the difficulty in oxidizing the adsorbed residues of ethanol (e.g. Pt-OCH_2CH_3, Pt-CHOH-CH_3, $(Pt)_2$-COH-CH_3, Pt-$COCH_3$, and Pt=C=O) at low potentials [26]. It was reported that the anodic peak appears in the reverse potential scan is attributed to the oxidation (removal) of the incomplete oxidized carbonaceous residues produced in the forward scan [27]. Therefore, the forward anodic current density (I_f) to the reverse anodic peak current density (I_b) ratio can be utilized to demonstrate the tolerance of the catalyst to the carbonaceous species accumulation [27]. For example, a catalyst with high (I_f/I_b) ratio is effectively capable of oxidizing alcohol to carbon dioxide during the anodic scan, thus minimizing the carbonaceous residues accumulation on the catalyst surface. Therefore, from the result shown in Fig. 4, the ratio is 4.8 and 7.2 for 400 and 600 nm Pt nanorods, respectively, while it is around 2.5 for Pt/C. Compared to Pt/C catalyst, such a high ratio for Pt nanorods reflects the enhanced electrocatalytic activity in terms of oxidizing a relatively larger amount of intermediate carbonaceous species to carbon dioxide in the forward scan. On the other hand, from a comparison of results in Fig. 4, it can be clearly seen that Pt nanorod electrocatalysts can reduce oxygen to water at a more positive potential (0.56 V) than that of the Pt/C (0.44 V), indicating that our catalyst has a lower oxygen overpotential.

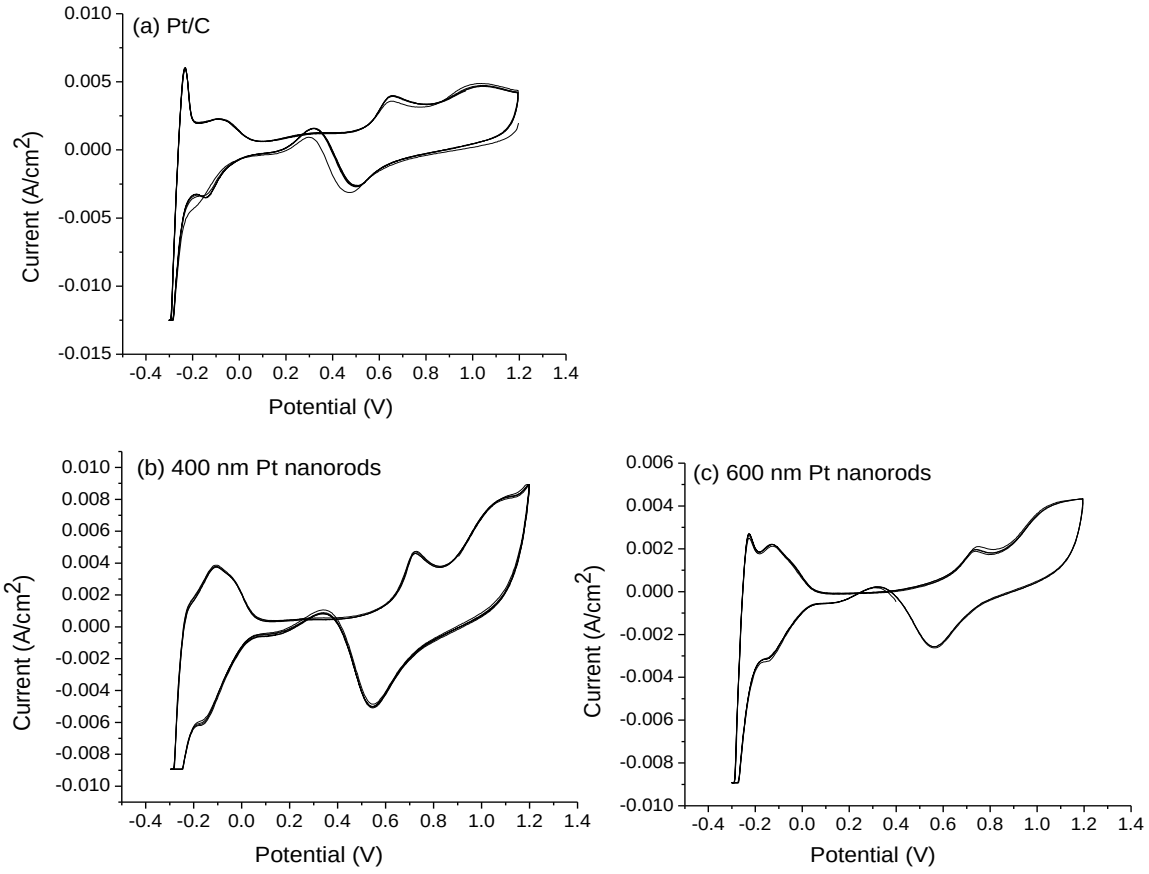

Figure 4. Room temperature cyclic voltammetry (CV) results of (a) a conventional carbon supported Pt nanoparticles (Pt/C), and single crystal GLAD Pt nanorod arrays of lengths (b) 400 nm, (c) 600 nm are shown. The Working electrodes were scanned between -300 to 1200 mV vs. SCE at a scan rate of 50 mV/s in 0.5 M H_2SO_4 and 0.5 M ethanol electrolyte.

The enhanced electrochemical activity of Pt nanorods for ORR and ethanol adsorption and electrooxidation is believed to be mainly due to the single-crystal property, the enhanced electrode porosity, and the dominance of the preferred crystal orientation for ethanol adsorption and electooxidation as well as ORR. Therefore, we believe that the results of this work have the potential to result in a significant advance in DAFC catalysis.

4. CONCLUSION

The CV measurements have been carried out to investigate the electrochemical properties of carbon-free, single layer, low-loading, and single-crystal Pt nanorod arrays as a novel electrocatalyst for direct ethanol fuel cells. A glancing angle deposition technique has been used to fabricate Pt nanorod arrays with different lengths. As confirmed by SEM images, the single crystal property of the individual Pt nanorods and their resistance to surface oxidation is believed to be the main reason for the enhanced electrochemical activity of Pt nanorods. The XRD results show that Pt nanorods are mainly oriented in Pt(100) which has the highest activity for ethanol adsorption and electrooxidation. The CV results imply that the I_f/I_b ratio is higher for Pt nanorods than that of Pt/C, indicating a slightly larger quantity of intermediate carbonaceous species is converted (oxidized) to carbon dioxide in the forward scan compared to Pt/C. On the other hand, our CV profiles also reveal that our catalyst is electrochemically more active for ORR than the conventional Pt/C electrocatalyst by reducing oxygen to water at more positive potential than that of Pt/C catalyst. The enhanced electrochemical activity of Pt nanorods for ethanol adsorption and electrooxidation and ORR is due to the single-crystal property, the enhanced electrode porosity and the dominance of the preferred crystal orientation for ethanol adsorption and electooxidation. These observations are encouraging and will lead us to continue this work by incorporating other material (Rh or Ir and SnO_2) with Pt, utilizing GLAD technique, to enhance the electrochemical activity and kinetics of ethanol oxidation reaction and overcome the major deficiency of elemental Pt catalyst; the catalyst poisoning problem, which caused by the accumulation of intermediate carbonaceous species on the catalyst surface during the anodic scan.

ACKNOWLEDGEMENTS
The authors would like to thank the UALR Nanotechnology Center and Dr. Fumiya Watanabe for his continued support in performing SEM and XRD measurements.

References

1. H. Li, G. Sun, L. Cao, L. Jiang and Q. Xin, *Electrochimica Acta*, 52 (2007) 6622.
2. S. C. S. Lai and M. T. M. Koper, *Faraday Discussion*, 140 (2008) 399.
3. E. Antolini, *Journal of Power Sources*, 170 (2007) 1.
4. L. Jiang, G. Sun, Z. Zhou, W. Zhou and Q. Xin, *Catalysis Today*, 93-95 (2004) 665.
5. C. Lamy, S. Rouddeau, E. M. Belgsir, C. Coutanceau and J. M. Leger, *Electrochimica Acta*, 49 (2004) 3901.

6. F. Delime, J. M. Leger and C. Lamy, *J. Appl. Electrochem*., 28 (1998) 27.
7. W. J. Zhou, S. Q. Song, W. Z. Li, G.Q. Sun, Q. Xin, S. Kontou, K. Pouhanitis and P. Tsiakaras, *Solid State Ionics*, 175 (2005) 797.
8. Y. Wang, S. Zou and W. B. Cai, *Catalysts*, 5 (2015) 1507.
9. L. Colmenares, H. W.ang, Z. Jusys, L. H. Jiang, S. Y. Yan, G. Q. Sun and R. J. Behm, *Electrochimica Acta*, 52 (2006) 221.
10. A. Kowal, M. Li, M. Shao, K. Sasaki, M. B. Vukmirovic, J. Zhang, N. S. Marinkovic, P. Liu, A. I. Frenkel and R. R. Adzic, *Nature Materials*, 8 (2009) 325.
11. M. Li, D. A. Cullen, K. Sasaki, N. S. Marinkovic, K. More and R. R. Adzic, *J. Am. Chem. Soc.*, 135 (2013) 132.
12. E. Higuchi, T. Takase, M. Chiku and H. Inoue, *J. Power Sources*, 263 (2014) 280.
13. T. S. Almeida, A. R. Van Wassen, R. B. Van Dover, A. R. De Andrade and H. D. Abruna, J. Power Sources, 284 (2015) 623.
14. W. J. Khudhayer, N. N. Kariuki, X. Wang, D. J. Myers, A. U. Shaikh and T. Karabacak, *J. Electrochem. Soc.* 158 (2011) B1029.
15. N. N. Kariuki, W. J. Khudhayer, T. Karabacak and D. J. Myers, *ACS Catalysis* 3 (2013) 3123.
16. W. J. Khudhayer, N. N. Kariuki, D. J. Myers, A. U. Shaikh and T. Karabacak, T., *J. Electrochem. Soc.*, 159 (2012) B729.
17. W. J. Khudhayer, M. Begum, U. B. Nasini, M. F. Cansizoglu, M. Yurukcu, A. U. Shaikh and T. Karabacak, *J.Appl. Electrochem.,*, 45 (2015) 1113.
18. T. Karabacak and T. M. Lu, *Handbook of Theoretical and Computational Nanotechnology*, edited by M. Rieth and W. Schommers (American. Scientific Publishers, Stevenson Ranch, CA), chap. 69 (2005) 729.
19. T. Karabacak, G. C. Wang and T. M. Lu, *J. Vac. Sci. Technol.*, A22 (2004) 1778.
20. E. Higuchi, H. Uchida and M. Watanabe, *J. Electroanal. Chem.*, 583 (2005) 69.
21. T. Karabacak, J. S. DeLuca, D. Ye, P. I. Wang, G. C. Wang, T. M. Lu, *J. Appl. Phys.*, 99 (2006) 064304.
22. W. J. Khudhayer, A. U. Shaikh and T. Karabacak, *Advanced Science Letters*, 4 (2011) 3551.
23. N. M. Markovic, H. A. Casteiger and P. N. Ross, *Journal of Physical Chemistry*, 99 (1995) 8290.
24. Y. H. Shih, G. V. Sagar, S. D. Lin, *J. Phys. Chem.*, 112 (2008) 123.
25. X. H. Xia, H. D. Liess and T. Iwasita, *J. Electroanal. Chem.*, 437 (1997) 233.
26. T. Iwasita and E. Pastor, *Electrochimica Acta*, 39 (1994) 531.
27. R. Monahara and J. B. Goodenough, *J. Mater. Chem*., 2 (1992) 875.